

Analytical Diagnosis and Tuning of Narrowband Multicoupled Resonator Filters

Wei Meng and Ke-Li Wu, *Senior Member, IEEE*

Abstract—A novel analytical filter diagnosis technique based on the partial fraction expansions of admittance matrix is proposed in this paper. The technique is applicable to computer-aided filter tuning of a general Chebyshev filter. The key issue in the proposed technique is the extension of the realizability conditions to the asynchronously tuned filters for removing the phase-loading effect. Using this analytical diagnosis technique, the inherent dispersion effects of the resonators and coupling elements are compensated by removable stray couplings in the diagnosed filter models. The filter topology that can be handled by this technique is only limited by the availability of the exact filter synthesis technique with which the filter to be diagnosed is designed.

Index Terms—Computer-aided tuning, filter diagnosis, filters, filter synthesis.

I. INTRODUCTION

MICROWAVE filters incorporating the generalized Chebyshev class of filtering functions have found wide applications in both satellite and terrestrial communication systems. A great deal of effort has been made over the past three decades in analytically synthesizing the filter coupling matrix according to an adequate topology with an optimal cost model. The most recent representative work in this subject would be Cameron's papers [1], [2].

For a given coupling matrix and filter topology, physical realization of a filter would largely depend on a costly and experience-based tuning. The core task in filter tuning is a diagnosis of the filter coupling status that corresponds to the current filter response. By comparing the designed circuit model and parameters (i.e., coupling matrix) against the diagnosed ones, the tuning direction and magnitude can be easily decided. Note that the diagnosed parameters must have relevance with those of the designed.

The computer-aided diagnosis and tuning of coupled resonator filters have been an active topic in the filter society for over ten years. The main driving force to the activities is the continuous demand on reducing the manufacturing cost and development cycle for various filter markets. The existing computer diagnosis techniques are mainly based on nonlinear optimization [3]–[5] in which different optimization strategies and schemes for parameter extraction are explored. In addition, analytical models based on the locations of system zeros and

poles [6]–[8] and artificial knowledge-based techniques [9] have also been investigated. The existing analytical models provide a recursive procedure to determine individual resonant frequencies and, consequently, inter-resonator couplings for highly restricted filter topologies [6], [7]. The existing techniques based on nonlinear optimization and artificial knowledge are of the nature of curve fitting. Due to the discrepancy in dispersion models between the theoretic and practical filters, if the coupled resonator circuit model is used in filter design and diagnosis, people should not be able to find an “exact” match between the extracted/diagnosed filter model and the designed filter model by a way of curve fitting.

In this paper, a systematic technique is proposed to approximately diagnose filter parameters based on a given filter topology and the measured scattering parameters $[S]$. No extra calibrations are needed to determine the loading effect. The filter topology that can be handled by this technique is only limited by the availability of the exact filter synthesis technique with which the filter to be diagnosed is designed.

The “approximation” introduced in the technique mainly comes from the forfeiture of the dispersion information and dissipation loss when converting a practical filter response to an ideal circuit model response. This loss of information is due to the imperfectness of the theoretic circuit model and is indispensable in a diagnosis. Being aware of the fact, an accurate determination of current coupling status would be a matter of tradeoff. The validation of the proposed technique is guaranteed by evaluating the poles and residues of the partial fraction expansions of the admittance matrix according to the multicoupled resonator filter network with the extended realizability conditions. Similar to any other diagnosis techniques, the phase loading at the filter ports must be assessed before a correct model can be extracted.

In this paper, the newly extended realizability conditions and the basic theory for removing the phase loading and diagnosing a filter response are discussed in Section II. Two examples are demonstrated in Section III showing the validation of the proposed technique. An application of this diagnosis technique of tuning a six-pole circular waveguide dual-mode filter is given in Section IV. Conclusions are then presented in Section V.

II. BASIC THEORY

The basic idea of the proposed diagnosis technique is very simple. By knowing the filter response in terms of scattering parameters $[S]$ and, consequently, admittance parameters $[Y]$, the partial fraction expansions of the admittance matrix $[Y]$ can be determined by finding the poles λ_k ($k = 1, 2, \dots, n$) that are common to all elements of the admittance matrix, and evaluating

Manuscript received December 19, 2005.

The authors are with the Department of Electronic Engineering, The Chinese University of Hong Kong, Shatin, Hong Kong (e-mail: kluw@ee.cuhk.edu.hk).

Color versions of Figs. 3–6, 9, 11, and Table V are available online at <http://ieeexplore.ieee.org>.

Digital Object Identifier 10.1109/TMTT.2006.881623

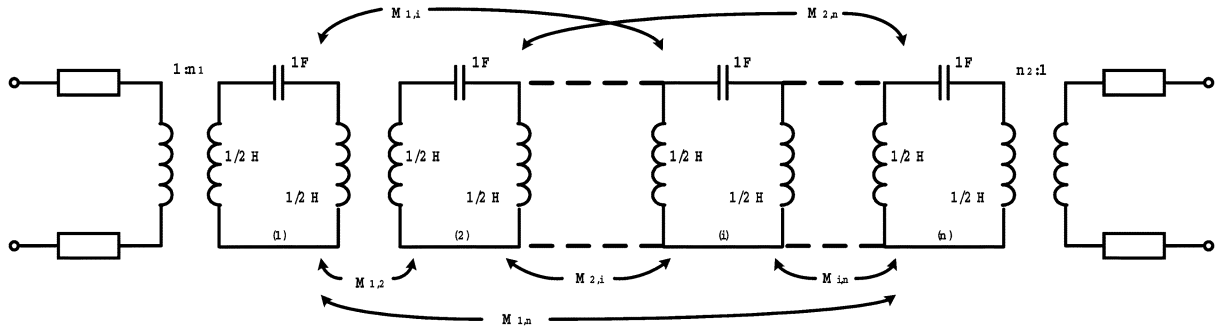


Fig. 1. Multicoupled resonator network with phase-loading effect.

all the residues ($r_{11k}, r_{12k}, r_{21k}, r_{22k}$) corresponding to every pole. The admittance matrix can now be expressed as

$$Y(s) = \begin{bmatrix} y_{11} & y_{12} \\ y_{21} & y_{22} \end{bmatrix} = \sum_{k=1}^n \frac{1}{s - j\lambda_k} \begin{bmatrix} r_{11k} & r_{12k} \\ r_{21k} & r_{22k} \end{bmatrix} \quad (1)$$

where s is the complex frequency variable.

Theoretically, having obtained the admittance matrix $[Y]$ from measured data, the coupling matrix corresponding to the filter response and the filter coupling topology can be recovered by the well-known transversal coupling matrix construction and a series of rotations to the coupling matrix. The resultant coupling matrix would comply with the given filter coupling topology [1], [2].

However, before the measured data is used in the diagnosis process, the phase-loading effect must be removed from the data so that all the system poles will appear on the real frequency axis and at the correct positions. Fig. 1 shows a general two-port multicoupled resonator network with a phase-loading effect.

The phase-loading effect refers to the discrepancy of the reference phase measured from an available reference plane at a filter port in measurement and the reference phase at a port of an ideal coupled resonator filter model. The phase loading may comprise several parts, which are: 1) the discrepancy of the reference phase plane between an ideal circuit model and a practical network; 2) the dispersion effect of the input/output coupling element; and 3) an extra length of transmission line introduced in measurement. Therefore, this loading effect must be assessed by the realizability conditions of the multicoupled resonator filter model [10], which is the fundamental model in the synthesis of this class of filters.

In [10], the realizability conditions of a synchronously tuned filter states that for an admittance matrix $[Y]$ to be expressed by the partial fraction expansions as (1), the following homogeneous conditions are necessary and sufficient:

$$\sum_{k=1}^n \lambda_k = 0 \quad (2a)$$

$$\sum_{k=1}^n \lambda_k r_{11k} = \sum_{k=1}^n \lambda_k r_{22k} = 0 \quad (2b)$$

$$\sum_{k=1}^n r_{21k} = 0. \quad (2c)$$

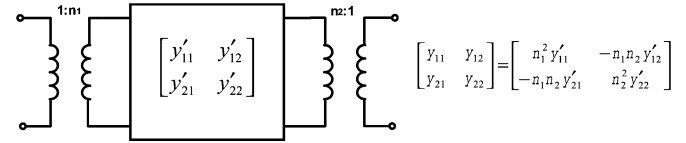


Fig. 2. Inner network with transformers.

It can be shown that the realizability conditions can be extended to an asynchronously tuned case in which the poles are still simple and purely imaginary. However, the right-hand-side conditions in (2a) and (2b) are no longer zero, but a small real number. The extended realizability conditions serve a critical role in gauging the phase-loading effect in the proposed diagnosis technique.

The admittance parameters of the inner network, as shown in Fig. 2, can be derived as [10]

$$y'_{21}(s) = [jM + sI]_{N1}^{-1} \quad (3a)$$

$$y'_{22}(s) = [jM + sI]_{NN}^{-1} \quad (3b)$$

where $[M]$ is an $N \times N$ reciprocal coupling matrix and $[I]$ is the identity matrix. Since $[M]$ is real and symmetric about its principal diagonal, all of its eigenvalues are real. Thus, it can be decomposed as

$$-M = T\Lambda T^t \quad (4a)$$

where

$$\Lambda = \text{diag}[\lambda_1, \lambda_2, \dots, \lambda_n] \quad (4b)$$

$$T T^t = I. \quad (4c)$$

and $[T]$ is a real orthogonal matrix with rows of orthogonal unit vectors. Consequently,

$$\begin{aligned} [jM + sI]^{-1} &= [-jT\Lambda T^t + sI]^{-1} \\ &= T \text{diag}\left[\frac{1}{s - j\lambda_1}, \dots, \frac{1}{s - j\lambda_n}\right] T^t. \end{aligned} \quad (5)$$

Relating (3) and (5) yields

$$y'_{21} = \sum_{k=1}^n \frac{T_{nk} T_{1k}}{s - j\lambda_k} \quad (6a)$$

$$y'_{22} = \sum_{k=1}^n \frac{T_{nk}^2}{s - j\lambda_k}. \quad (6b)$$

By the formula given in Fig. 2, the admittance parameters of a network with transformers can be derived as

$$y_{21} = -n_1 n_2 y'_{21} = -n_1 n_2 \sum_{k=1}^n \frac{T_{nk} T_{1k}}{s - j\lambda_k} \quad (7a)$$

$$y_{22} = n_2^2 y'_{21} = n_2^2 \sum_{k=1}^n \frac{T_{nk}^2}{s - j\lambda_k}. \quad (7b)$$

Now the conditions given in (2) for synchronously tuned case can be extended to asynchronously tuned case. For condition (2a), the trace of coupling matrix $[M]$ is the sum of its eigenvalues. While, in general, the trace of $[M]$ in the asynchronously tuned case is not zero as follows:

$$\sum_{k=1}^n \lambda_k = \text{trace}(M). \quad (8a)$$

Equating y_{22} in (1) and (7b), the product sum of the eigenvalue and residue in (2b) can be deduced as

$$\sum_{k=1}^n \lambda_k r_{22k} = \sum_{k=1}^n \lambda_k n_2^2 T_{nk}^2 = n_2^2 \sum_{k=1}^n \lambda_k T_{nk}^2 = n_2^2 M_{nn}. \quad (8b)$$

Note here that the coupling matrix is defined in (4a). Since $[T]$ is an orthogonal matrix, the sum of the residues in (2c) can be deduced as

$$\sum_{k=1}^n r_{21k} = \sum_{k=1}^n -n_1 n_2 T_{nk} T_{1k} = (-n_1 n_2) \sum_{k=1}^n T_{nk} T_{1k} = 0. \quad (8c)$$

In this proposed diagnosis technique, the amount of phase loading is gauged by evaluating the above extended realizability conditions. Having had the phase-loading effect removed, the locations of the poles λ_k can be identified along the real frequency axis. According to (1), we can have a set of over sampled linear equations from the measured data in a matrix form as follows:

$$\begin{bmatrix} y(f_1) \\ y(f_2) \\ \vdots \\ y(f_m) \end{bmatrix} = \begin{bmatrix} \frac{1}{f_1 - \lambda_1} & \frac{1}{f_1 - \lambda_2} & \cdots & \frac{1}{f_1 - \lambda_n} \\ \frac{1}{f_2 - \lambda_1} & \cdot & \cdot & \cdot \\ \vdots & \cdot & \cdot & \cdot \\ \frac{1}{f_m - \lambda_1} & \cdot & \cdot & \frac{1}{f_m - \lambda_n} \end{bmatrix} \begin{bmatrix} r_1 \\ r_2 \\ \vdots \\ r_n \end{bmatrix} \quad (9)$$

$$\{y_m\} = [A] \cdot \{r_n\}.$$

The residue vector can be solved in the least square sense

$$\{r_n\} = ([A]^T \cdot [A])^{-1} \cdot [A]^T \cdot \{y_m\}. \quad (10)$$

Thus far, all poles λ_k and residues r_{21k} and r_{22k} can be determined by the above-mentioned equations. By the well-known coupling matrix construction and a series of matrix rotation [1],



Fig. 3. Four-pole circular waveguide dual-mode filter.

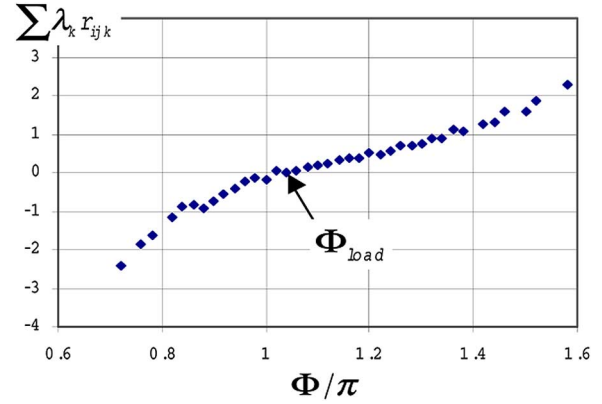


Fig. 4. Product sum of eigenvalue and residue versus loading phase diagram for the dual-mode filter.

the coupling matrix corresponding to the current filter response conformed in a certain topology can be recovered. Actually, filter tuning is an iterative process of filter diagnosis. Each of the diagnosis recovers the current filter coupling status of a physical filter structure in a tuning process. By comparing the designed coupling matrix against the diagnosed one, the tuning direction and magnitude can be easily determined.

III. EXAMPLES OF FILTER DIAGNOSIS

As the first example, a fourth-order circular waveguide dual-mode filter is simulated using a full-wave electromagnetic (EM) modal analysis program, which has been fully verified by experiments. The filter consists of two circular cavities that are separated by a cross iris. As shown in Fig. 3, a tuning tooth is stuck out at the middle of each cavity; one is at 45° and the other is at -45° . In this modal analysis, a certain surface impedance is considered ($\sigma = 2.0E + 7$ S/m) to emulate a cavity of $Q = 8000$. The reference planes in the EM simulation are defined at the outer surfaces of the input and the output irises.

Before the filter is diagnosed, an appropriate phase loading must be removed from the “measured” S -parameters. As discussed in Section II, the value of the product sum of eigenvalue λ_k and residue r_{ijk} ($\sum \lambda_k r_{ijk}$) is used as a criteria to determine the phase loading Φ_{load} . For this example, the function of $\sum \lambda_k r_{ijk}$ versus loading phase is plotted in Fig. 4 from which an appropriate phase-loading angle $\Phi_{load} = 1.044\pi$ (rad) can be found. It is worth mentioning that an appropriate phase-loading angle is not very sensitive to the final result. A variation of few degrees will not change the result significantly.

In fact, the influence of the phase loading can also be reflected in the responses of the admittance $[Y]$ from which the poles' locations and the residues of the partial fraction expansions are

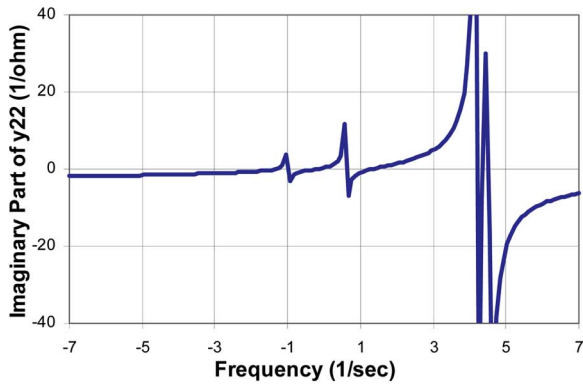


Fig. 5. Imaginary part of y_{22} before the phase loading is removed.

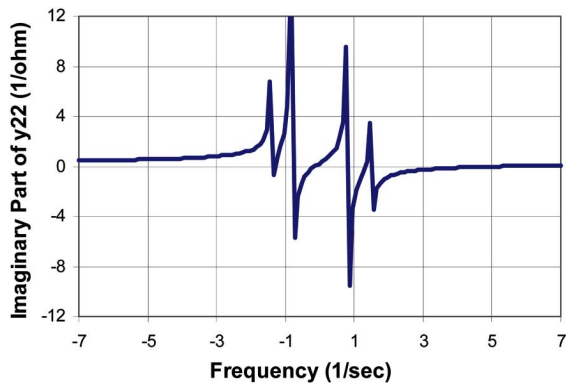


Fig. 6. Imaginary part of y_{22} after the phase loading is removed.

TABLE I
DIAGNOSED COUPLING MATRIX OF THE DUAL
MODEL FILTER WITH STRAY COUPLINGS

	S	1	2	3	4	L
S	0	1.2309	0	0	0	0
1	1.2309	0.0317	1.0159	0	-0.1989	0.0127
2	0	1.0159	-0.0649	0.8447	-0.0061	0
3	0	0	0.8447	-0.0645	0.9967	0
4	0	-0.1989	-0.0061	0.9967	-0.0054	1.2011
L	0	0.0127	0	0	1.2011	0

determined. The plots of the imaginary part of the y_{22} before and after removing the phase loading are illustrated in Figs. 5 and 6, respectively. Of course, the real part of $[Y]$ -parameters also exists due to the finite conductor loss.

With the eigenvalues and residues determined, the diagnosed coupling matrix can be determined using the same procedure by which the filter can be synthesized through a series of matrix rotations. The directly diagnosed coupling matrix of the dual-mode filter is listed in Table I, where the center frequency is $f_0 = 12.18$ GHz and the bandwidth is $BW = 60$ MHz. The filter response from the diagnosed couplings and the original EM simulated response are superposed in Fig. 7. Good correlation can be observed. Nevertheless, by examining Table I, two interesting phenomena that deviate from common sense can be noticed, which are: 1) the existence of weak stray couplings (M_{1L} and M_{24}) and 2) a small difference between the input coupling M_{S1} and output coupling M_{4L} . Being aware that a physical waveguide filter will not behave in the same way as

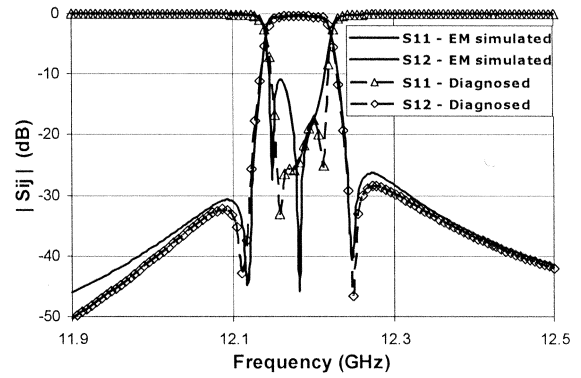


Fig. 7. Responses of the dual model filter: EM simulated and recovered with the diagnosed coupling matrix including stray coupling elements.

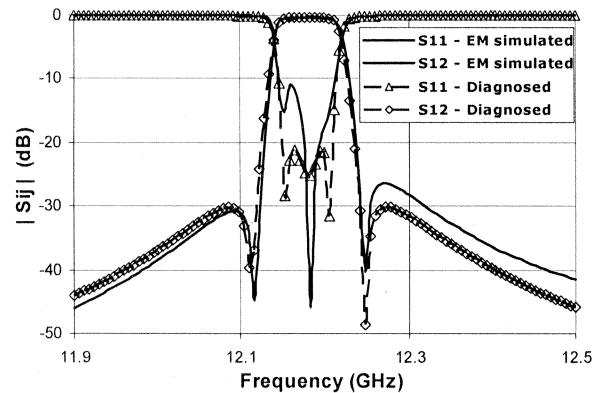


Fig. 8. Responses of the dual model filter: EM simulated and recovered with the diagnosed coupling matrix excluding stray coupling elements.

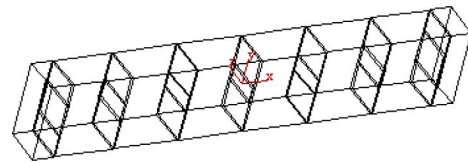


Fig. 9. Six-pole H -plane waveguide Chebyshev filter.

an ideal coupled resonator filter, all the coupling elements and resonators have dispersion. The dispersion is compensated by those removable stray couplings and the nonideal symmetry of the coupling matrix in the diagnosis. If the stray couplings are removed, as shown in Fig. 8, a reasonably good matching between the “measured” response and the diagnosed response can still be obtained.

The second example is a six-pole H -plane waveguide Chebyshev filter with waveguide dimensions of $0.75 \text{ in} \times 0.375 \text{ in}$. As shown in Fig. 9, six waveguide cavities are separated by seven rectangular irises. The reference planes are defined at the outer surfaces of the input and output irises. Again, the full-wave modal analysis program is used to simulate the filter response with surface conductivity of $2.0E + 7$ (S/m) that is equivalent to the filter cavities with $Q = 4000$.

The similar procedure is applied to the H -plane filter. The diagnosed coupling matrix is compared with the original designed coupling matrix in Table II, where $f_0 = 12.0$ GHz and $BW = 30$ MHz. It can be found that the largest error between

TABLE II
COMPARISON OF THE COUPLING COEFFICIENTS OF THE SIX-POLE *H*-PLANE WAVEGUIDE FILTER

Couplings	Designed	Diagnosed
M01	1.1014	1.0474
M11		0.0685
M12	0.9370	0.9160
M16		0.0312
M17		-0.0521
M22		-0.0340
M23	0.6460	0.6710
M25		-0.0421
M26		0.0445
M33		-0.0924
M34	0.6110	0.6251
M35		-0.0408
M44		0.0361
M45	0.6470	0.6655
M55		-0.0606
M56	0.9390	0.9088
M66		0.1081
M67	1.1027	1.0091

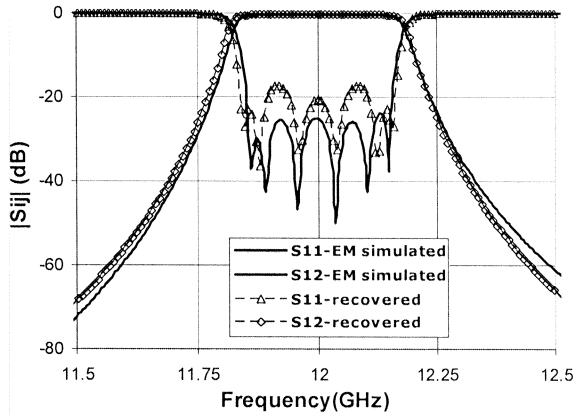


Fig. 10. Responses of the six-pole *H*-plane waveguide filter: EM simulated and recovered.

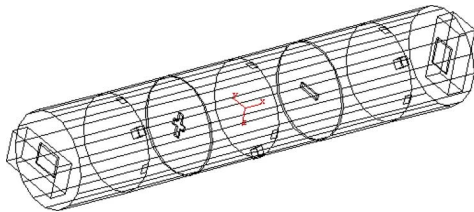


Fig. 11. Six-pole circular waveguide dual-mode filter.

the designed coupling elements and the diagnosed coupling elements is approximately 8%. The error is mainly caused by the inaccuracy of the pole location due to the presence of the conductor loss and dispersion effects. The most obvious dispersion effect in this example is the deviation in the rolloff slopes.

Due to the existence of the dispersion, the original diagnosed coupling matrix will come with some stray cross couplings. These unexpected cross couplings create some unwanted transmission zeros. Since there should not be any cross couplings for an *H*-plane waveguide filter, the stray couplings must be discarded. The response of the diagnosed filter, after the stray

TABLE III
SYNTHESIZED COUPLING MATRIX FOR SIXTH-ORDER DUAL-MODE FILTER IN FOLDED STRUCTURE

	S	1	2	3	4	5	6	L
S	0	1.0374	0	0	0	0	0	0
1	1.0374	0	0.8692	0	0	0	0	0
2	0	0.8692	0	0.6022	0	0.1189	0	0
3	0	0	0.6022	0	0.6851	0	0	0
4	0	0	0	0.6851	0	-0.6022	0	0
5	0	0	0.1189	0	-0.6022	0	0.8692	0
6	0	0	0	0	0	0.8692	0	1.0374
L	0	0	0	0	0	0	1.0374	0

TABLE IV
SYNTHESIZED COUPLING MATRIX FOR SIXTH-ORDER DUAL-MODE FILTER IN DUAL-MODE STRUCTURE

	S	1	2	3	4	5	6	L
S	0	1.0374	0	0	0	0	0	0
1	1.0374	0	0.8527	0	-0.1683	0	0	0
2	0	0.8527	0	0.7235	0	0	0	0
3	0	0	0.7235	0	0.5555	0	0	0
4	0	-0.1683	0	0.5555	0	-0.6139	0	0
5	0	0	0	0	-0.6139	0	0.8692	0
6	0	0	0	0	0	0.8692	0	1.0374
L	0	0	0	0	0	0	1.0374	0

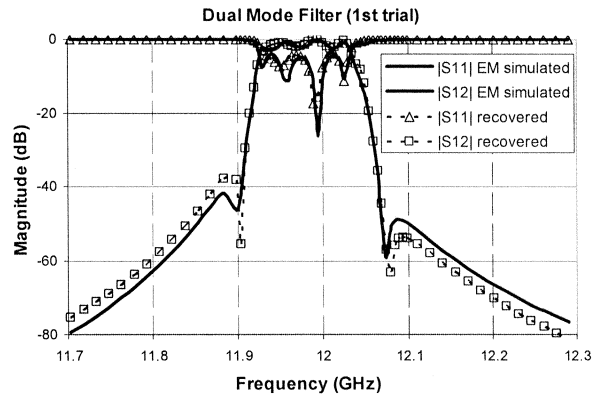


Fig. 12. Responses of the six-pole circular waveguide dual-mode filter (first trial): EM simulated and recovered.

couplings are removed, is compared with the original EM “measured” response in Fig. 10. Good correlation is observed.

IV. EXAMPLES OF FILTER TUNING

Here, a process of diagnosing and tuning a six-pole dual-mode filter is demonstrated with the aid of the proposed diagnosing technique.

The designed six-order dual-mode filter is physically realized in a circular waveguide and with two transmission zeros. The filter consists of three circular waveguide cavities that are separated by a cross iris and a rectangular iris, as shown in Fig. 11. Three tuning teeth are stuck out at the middle of each cavity, respectively. Due to the polarization of modes in circular waveguide, the orientation of input and output irises are different. The dimensions of input and output waveguide are 0.75 in × 0.375 in and the radius of the circular waveguide is 0.535 in. The same full-wave modal analysis program is used and surface conductivity of $2.0E + 7$ (S/m) is introduced to emulate a cavity of $Q = 8000$.

TABLE V
DIAGNOSED COUPLING MATRIX AFTER EACH TRIAL

	Designed	1st Trial	2nd Trial	3rd Trial	4th Trial	5th Trial	6th Trial
M_{01}	1.0374	0.952	0.9655	0.9604	0.9645	0.9514	0.9586
M_{11}	0	0.6263	0.2455	0.3432	0.2538	0.3043	-0.0672
M_{12}	0.8692	1.1781	0.9885	0.9524	0.9436	0.9315	0.8516
M_{22}	0	0.0865	-0.4755	-0.5134	-0.0756	-0.0303	-0.0327
M_{23}	0.6022	0.8586	0.4636	0.4819	0.5396	0.6486	0.6239
M_{25}	0.1189	0.1359	0.085	0.079	0.0751	0.1089	0.1409
M_{33}	0	0.4032	-0.1999	-0.2126	0.0088	-0.0499	0.0341
M_{34}	0.6851	0.8676	0.5707	0.6396	0.6868	0.6294	0.7151
M_{35}	0	0.0742	0.1004	0.1317	0.0602	0.0219	0.0094
M_{44}	0	0.5709	0.4039	0.26	0.1853	0.1051	0.0313
M_{45}	-0.6022	-0.7015	-0.7128	-0.498	-0.5249	-0.6043	-0.5985
M_{55}	0	0.6129	0.3671	-1.0037	0.0077	0.1196	0.0454
M_{56}	0.8692	1.2187	0.9704	0.9911	0.8941	0.9095	0.8943
M_{66}	0	1.3377	1.1259	-0.0203	-0.1486	-0.1816	-0.0822
M_{67}	1.0374	0.9475	0.9594	0.9756	0.9683	0.959	0.9626

Two synthesis steps are necessary to obtain the required coupling matrix for the dual-mode circular waveguide filter. The coupling matrix of a folded structure for the required filter characteristic is synthesized first by a standard technique [1] and is given in Table III. A further rotation is applied on the folded coupling matrix to derive the final coupling matrix, which is listed in Table IV, for the dual-mode realization [11]. According to the elements in the coupling matrix of dual-mode realization, the initial dimensions of the circular waveguide dual-mode filter are determined by following the guideline discussed in [12]. In fact, the design dimensions concerned in the initial design are also those to be adjusted in the tuning process.

Applying the proposed diagnosis technique, the responses of the diagnosed filter, after removing the unnecessary stray couplings, are compared with the EM simulated responses of the first trial in Fig. 12. Good correlation shows the correctness of diagnosed coupling matrix. The diagnosed folded coupling matrix is then listed in Table V altogether with the designed folded coupling matrix.

By knowing the differences of the designed and diagnosed coupling matrix, the tuning direction and magnitude of physical structures could be decided by employing the space-mapping technique [13].

With indication of the elements being altered by arrows, Table V records the changes of the folded coupling matrix in six tuning iterations. The responses of the recovered coupling matrix are superposed with the EM “measured” response of the last iteration in Fig. 13. The EM responses are also compared with those of the designed filter model in Fig. 14, showing the success of tuning process. By the nature of the proposed diagnosis technique, the diagnosed coupling matrix is an approximation to the designed coupling matrix because of the dispersions. Being aware of very high sensitivity of in-band return loss, a fine tuning using nonlinear optimization can be applied to tune the filter to the desired response.

By examining the data in Table V, several points must be addressed here. The discrepancy between the input and output couplings with the targeted values, which has been stated in Section III, has always existed, especially for M_{01} . By admitting this discrepancy, the tuning process can still be carried on. The

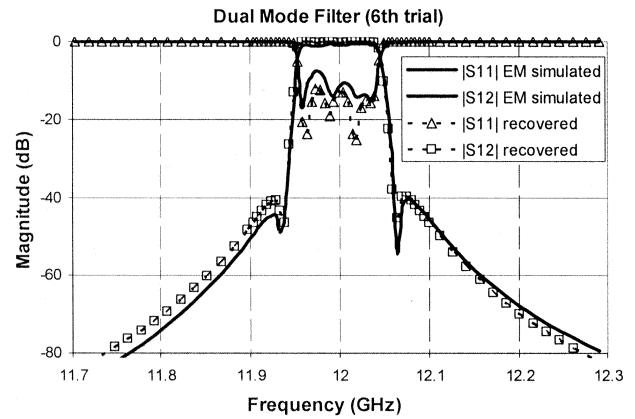


Fig. 13. Responses of the six-pole circular waveguide dual-mode filter (sixth trial): EM simulated and recovered.

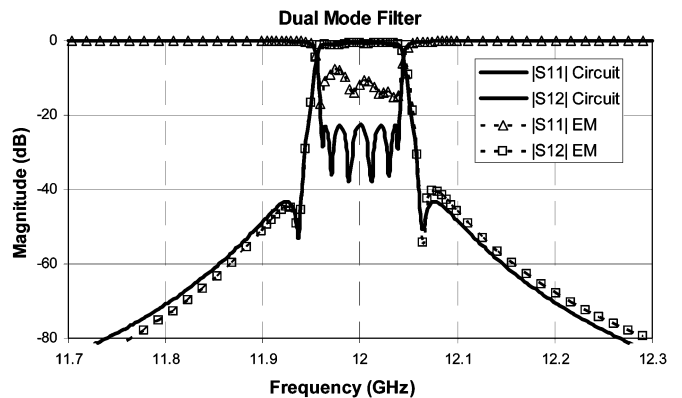


Fig. 14. Responses of the six-pole circular waveguide dual-mode filter (sixth trial): EM simulated and designed.

cause of this discrepancy may be due to the dispersion. Another interesting point is that the coupling M_{35} always exists in the diagnosed coupling matrix and it cannot be eliminated as stray coupling, but as the diagnosed coupling matrix approaches the synthesized one, in which the coupling M_{35} is zero, this coupling becomes smaller and converges automatically.

V. CONCLUSIONS

An analytical filter diagnosis technique has been proposed and demonstrated through a number of practical filter examples. The technique can systematically extract the coupling matrix for a given general Chebyshev filter topology and measured S -parameters without any prior knowledge. By extending the realizability conditions to an asynchronously tuned filter case, the criteria for removing the phase-loading effect has also been developed and verified.

Due to the inevitable dispersion in practical filters, as any other filter diagnosis techniques, the proposed diagnosis model is not "exact." It may generate certain removable weak stray couplings to compensate the dispersion. Nevertheless, the omission of the stray couplings will still lead the diagnosed parameters to a very good starting point to a more specific filter parameter extraction using nonlinear optimization by which the dispersion is absorbed into the coupling coefficients.

ACKNOWLEDGMENT

The authors would like to thank the encouragement to this research from Dr. G.-C. Liang, Allrizon Tongguang Communications Equipment Company Ltd., Shanghai, China, and Dr. G. McDonald, Andrew (ShenZhen) Ltd., Shenzhen, China.

REFERENCES

- [1] R. J. Cameron, "General coupling matrix synthesis methods for Chebyshev filtering functions," *IEEE Trans. Microw. Theory Tech.*, vol. 47, no. 4, pp. 433–442, Apr. 1999.
- [2] —, "Advanced coupling matrix synthesis techniques for microwave filters," *IEEE Trans. Microw. Theory Tech.*, vol. 51, no. 1, pp. 1–10, Jan. 2003.
- [3] P. Harscher, R. Vahldieck, and S. Amari, "Automated filter tuning using generalized low-pass prototype networks and gradient-based parameter extraction," *IEEE Trans. Microw. Theory Tech.*, vol. 49, no. 12, pp. 2532–2538, Dec. 2001.
- [4] G. Pepe, F.-J. Gortz, and H. Chaloupka, "Computer-aided tuning and diagnosis of microwave filters using sequential parameter extraction," in *IEEE MTT-S Int. Microw. Symp. Dig.*, 2004, pp. 1373–1376.
- [5] M. Yu and W.-C. Tang, "A fully automated filter tuning robots for wireless basestation duplexers," presented at the IEEE MTT-S Int. Microwave Symp. Workshop, 2003, presentation.
- [6] H.-T. Hsu, H.-W. Yao, K. A. Zaki, and A. E. Atia, "Computer-aided diagnosis and tuning of cascaded coupled resonators filters," *IEEE Trans. Microw. Theory Tech.*, vol. 50, no. 4, pp. 1137–1145, Apr. 2002.
- [7] H.-T. Hsu, Z. Zhang, K. A. Zaki, and A. E. Atia, "Parameter extraction for symmetric coupled-resonator filters," *IEEE Trans. Microw. Theory Tech.*, vol. 50, no. 12, pp. 2971–2978, Dec. 2002.
- [8] W. Meng and K.-L. Wu, "An analytical diagnosis of general Chebyshev narrowband coupled resonator filters," in *Proc. Asia-Pacific Microw. Conf.*, 2005, pp. 2180–2183.

- [9] V. Miraftab and R. R. Mansour, "Computer-aided tuning of microwave filters using fuzzy logic," *IEEE Trans. Microw. Theory Tech.*, vol. 50, no. 12, pp. 2781–2788, Dec. 2002.
- [10] A. E. Atia, A. E. Williams, and R. W. Newcomb, "Narrow-band multiple-coupled cavity synthesis," *IEEE Trans. Circuits Syst.*, vol. CAS-21, no. 9, pp. 649–655, Sep. 1974.
- [11] R. J. Cameron and J. D. Rhodes, "Asymmetric realizations for dual-mode bandpass filters," *IEEE Trans. Microw. Theory Tech.*, vol. MTT-29, no. 1, pp. 51–58, Jan. 1981.
- [12] K.-L. Wu, "An optimal circular-waveguide dual-mode filter without tuning screws," *IEEE Trans. Microw. Theory Tech.*, vol. 47, no. 3, pp. 271–276, Mar. 1999.
- [13] J. W. Bandler, R. M. Biernacki, S. H. Chen, R. H. Hemmers, and K. Madsen, "Electromagnetic optimization exploiting aggressive space mapping," *IEEE Trans. Microw. Theory Tech.*, vol. 43, no. 10, pp. 2874–2882, Oct. 1995.



Wei Meng received the B.Eng. degree (with first-class honors) and M.Phil. degree in electronic engineering from The Chinese University of Hong Kong, Hong Kong, in 2003 and 2005, respectively.

He is currently a Research Assistant with the Department of Electronic Engineering, The Chinese University of Hong Kong. His research is focused on the modeling and design of passive microwave components, especially on the synthesis and design techniques of microwave filters.



Ke-Li Wu (M'90–SM'96) received the B.S. and M.Eng. degrees from Nanjing University of Science and Technology, Nanjing, China, in 1982 and 1985, respectively, and the Ph.D. degree from Laval University, Quebec, QC, Canada, in 1989.

From 1989 to 1993, he was with the Communications Research Laboratory, McMaster University, Montreal, QC, Canada, as a Research Engineer and a Research Group Manager. In March 1993, he joined the Corporate Research and Development Division, Com Dev International, where he was a Principle Member of Technical Staff in charge of developing advanced EM design software for various microwave subsystems for communication satellites and wireless communications. Since October 1999, he has been with the Department of Electronic Engineering, The Chinese University of Hong Kong, Hong Kong, where he is a Professor. He has authored or coauthored numerous publications in the areas of EM modeling and microwave and antenna engineering. He holds one Canadian patent and one U.S. patent. He contributed to *Finite Element and Finite Difference Methods in Electromagnetics Scattering* (Elsevier, 1990) and *Computational Electromagnetics* (Elsevier, 1991). His current research interests include all the aspects of numerical methods in electromagnetics, various passive microwave circuits, integrated antenna arrays, low-temperature co-fired ceramic (LTCC) multichip modules (MCMs) for wireless communications, and active RF identification (RFID) systems.

Dr. Wu was the recipient of a 1992 URSI Young Scientist Award. He was also the recipient of the 1993 Industry Feedback Award presented by the Telecommunication Research Institute of Ontario, Canada, and the 1998 Com Dev Achievement Award.